PAPER

NJC
www.rsc.org/njc

EPR study of the magnetic states of a mixed-valence $V_4^{IV}V_2^{V}$ alkoxypolyoxovanadium cluster

Maria A. Augustyniak-Jablokow,[a] Serguei A. Borshch,[b] Charles Daniel,[c] Hans Hartl[c] and Yurii V. Yablokov*[a]

[a] *Institute of Molecular Physics PAN, Smoluchowskiego 17, 60-179 Poznan, Poland. E-mail: yablokov@ifmpan.poznan.pl; Fax: +48-61 86 84 524; Tel: +48-61 86 95 205*
[b] *Laboratoire de Chimie, UMR 5182 CNRS-Ecole Normale Supérieure de Lyon 46, allée d'Italie, 69364 Lyon Cedex 07, France. E-mail: Serguei.Borchtch@ens-lyon.fr; Fax: +33(0)4 72 72 88 60; Tel: +33(0)4 72 72 88 59*
[c] *Institut für Chemie/Anorganishe und Analitishe Chemie Freie Universität Berlin, Fabeckstrasse 34-36, 14195 Berlin, Germany. E-mail: hartl@chemie.fu-berlin.de; Fax: +49-30-838-52424; Tel: +49-30-838-54003/52416*

Received (in Durham, UK) 11th August 2004, Accepted 10th May 2005
First published as an Advance Article on the web 16th June 2005

The EPR studies of the hexanuclear vanadium cluster in a $[V_4^{IV}V_2^{V}O_7(OCH_3)_{12}]$ single crystal are reported. The spectrum of the mixed valence clusters consists of a single lorentzian line and additional signals in the magnetic field range ~240–440 mT and is observed in the 4.2–300 K temperature range. At about 190 K, on cooling, an abrupt change of the spectrum due to the structural phase transition, followed by a strong hysteresis, is discovered. Temperature dependence of the EPR spectra indicates an electron transfer between V^{IV} and V^{V}. Obtained results are discussed in the framework of the Heisenberg–Anderson–Zener Hamiltonian approach. The possibilities of other approaches is also considered.

DOI: 10.1039/b412427h

Introduction

Mixed-valence clusters in which transition metal ions with different electronic configurations occupy equivalent positions are of great interest for studying the interplay between exchange interactions and electron transfer. Two types of phenomena can be distinguished in such systems. The phenomena of one of these types take place when additional electrons are transferred between paramagnetic cores and is usually referred to as double exchange. The idea of double exchange originates from the early works of Zener, Anderson and Hasegawa.[1–3] It was applied to different polynuclear clusters of various nuclearity, especially to iron–sulfur clusters.[4–6] Another possibility appears when several electrons are transferred between non-magnetic cores. This delocalisation, together with the topology of the cluster, determines the energy spectrum of available spin states. This type of phenomena have been studied mainly in application to reduced polyoxometalates.[7–11]

Theoretical analysis of double-exchange systems in earlier studies was performed using model multi-electron or spin Hamiltonians.[2–4] Recently, quantum-chemical DFT and *ab initio* calculations have been used for these systems.[12,13] The magnetic states of reduced polyoxometalates have been investigated mainly within the valence bond approach. However, several applications of quantum-chemical methods are also known.[10,11]

Electron paramagnetic resonance is known to be a very useful instrument to study magnetic clusters,[14] providing information on both isotropic and anisotropic exchange interactions[15,16] and cluster dynamics.[17–19] However, examples of EPR investigation of magnetic clusters with delocalised electrons are quite rare.[20]

Recently, a new series of mixed-valence polyoxometalate clusters with methylated bridges of the general composition $[V_{6-n}{}^{IV}V_n^{V}O_7(OCH_3)_{12}]^{-(2-n)}$ ($n = 0$–3) have been synthesized.[21] Here, we present the EPR results for the $n = 2$ member of this series. Our results seem to indicate that the intramolecular electron transfer can play an important role in the formation of magnetic states of this cluster.

Experimental

$[V_4^{IV}V_2^{V}O_7OCH_3)_{12}]$ was synthesized according to the literature procedure.[21] Single crystals of the size and quality suitable for EPR study were obtained by recrystallization from hexane, and were then indexed using an optical goniometer.

The structure of $[V_4^{IV}V_2^{V}O_7(OCH_3)_{12}]$ (Fig. 1) was solved by X-ray diffraction† at 173 K. It crystallizes in the $Pna2_1$ space group, with four magnetically inequivalent clusters in the unit cell (Fig. 2) characterized by $a = 20.8643$ Å, $b = 10.083$ Å and $c = 13.5064$ Å. In each mixed-valence cluster $[V_4^{IV}V_2^{V}O_7(OCH_3)_{12}]$ containing four paramagnetic vanadium(+IV) and two diamagnetic vanadium(+V) nuclei, the six vanadium nuclei surround an oxo anion, forming a slightly distorted octahedron. The vanadium nuclei all equally bind one terminal oxygen atom

† Crystal structure determination of $[V_6O_7(OCH_3)_{12}]$: Bruker XPS diffractometer (CCD area detector, Mo-Kα radiation, $\lambda = 0.710\ 73$ Å, graphite monochromator), empirical absorption correction using symmetry-equivalent reflections (SADABS), direct methods, difference Fourier syntheses. The initial structures were refined against F^2 (Bruker-SHELXTL, version 5.1, 1998). The hydrogen atoms were calculated in geometrically idealised positions. *Crystal data*: $C_{12}H_{36}O_{19}V_6$, $M = 790.05$, space group $Pna2_1$, $a = 20.8343(12)$, $b = 10.0830(6)$, $c = 13.5064(8)$ Å, $V = 2837.3(3)$ Å^3, $Z = 4$, $T = 173(2)$ K, $\mu = 1.971$ mm^{-1}, number of independent reflections used = 7344, $R_{int} = 0.0317$, Final R values: $R1 = 0.0282$ ($I > 2\sigma(I)$), $wR2 = 0.0694$ ($I > 2\sigma(I)$). CCDC reference number 274087. See http://dx.doi.org/10.1039/b412427h for crystallographic data in CIF or other electronic format.

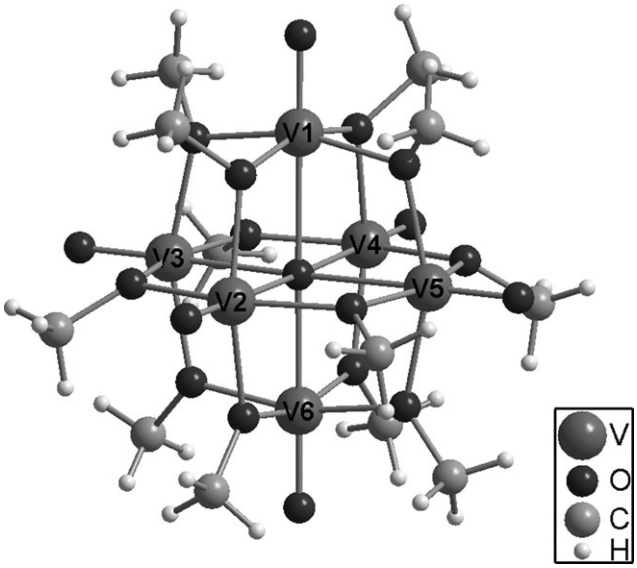

Fig. 1 The structure of alkoxypolyoxovanadium cluster.

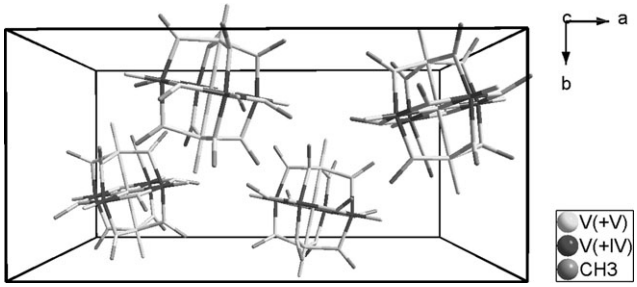

Fig. 2 An arrangement of the hexavanadium clusters in the unit cell of the $[V_4^{IV}V_2^{V}O_7(OCH_3)_{12}]$ crystal.

and four μ_2-bridging methoxo ligands, respectively (Table 1). Valence-sum calculations‡[22] indicate a clear magnetic order in the crystalline state at 173 K, the four paramagnetic vanadium(+IV) nuclei being arranged in an equatorial fashion (Fig. 1).

EPR spectra were measured on an X-band RADIOPAN spectrometer with OXFORD temperature equipment. The single crystals of $[V_4^{IV}V_2^{V}O_7\ (OCH_3)_{12}]$ were studied in the 300–4.2 K temperature interval. The size of the crystals did not exceed $1.2 \times 1.0 \times 0.5$ mm. The shape of the EPR spectrum and the positions of EPR signals depend on the temperature (Fig. 3) and the crystal orientation (Fig. 4). A predominant EPR line of a Lorentzian shape is accompanied by some weak signals. At 291 K these weak signals are observed at a constant magnetic field B in a direction close to the crystallographic axis b ([010] direction) at $B \approx 240$, 290, (350) and 410 mT (see Fig. 5). They are transformed into a broad signal at temperatures lower than 160 K (Fig. 3) and spread below 140–130 K. Their presence has been detected even at 4.2 K. Estimations show that the integral intensity of this "weak signal spectrum" reaches a maximum value in the range 190–140 K. The angular dependences of the line width ΔB of the predominant signal measured in the ab plane at 294 and 170 K are shown in Fig. 6. At 294 K, ΔB of the predominant EPR line takes a maximum value for the magnetic field B directed along the [010] axis (four magnetically inequivalent cluster-molecules are symmetrical relative to this direction and their V_1–O–V_6 axes deviate from

‡ The oxidation state of atom i is given by $\sum_j v_{ij} = V$ with $v_{ij} = \exp[(R_{ij} - d_{ij})/b]$. Here b is taken to be a 'universal' constant equal to 0.37 Å, v_{ij} is the valence of a bond between two atoms i and j, R_{ij} is the empirical parameter, and d_{ij} is the observed bond length.

Table 1 V–O bond lengths (Å) in $[V_6O_7(OCH_3)_{12}]$

	$V–O_{terminal}$	$V–O_{bridging}$	$V–O_{central}$
V1	1.5858	1.9043, 1.9201, 1.9223, 1.9265	2.3144
V2	1.597	1.9836, 1.9842, 2.0147, 2.0152	2.3046
V3	1.5914	1.9810, 1.9954, 2.0224, 2.0234	2.2971
V4	1.596	1.979, 1.980, 2.0043, 2.0153	2.3090
V5	1.5987	1.985, 1.9919, 2.0102, 2.0151	2.3043
V6	1.5811	1.908, 1.9188, 1.9263, 1.9294	2.2175

[010] only by $\sim 12°$), then reaches a minimum at an angle θ between B and [010] $\approx 54°$ and increases again to $\theta = 90°$. The positions of the maximum and intermediate ΔB values, measured at $T = 170$ K, have exchanged relative to [010] direction and the angular distance between the position of ΔB minimum and maximum is $\approx 54°$ again. The temperature dependences of the ΔB and g-factor of the EPR signal, recorded for the magnetic field B parallel to the [010] direction is presented in Fig. 7.

The nuclear spin of vanadium is $I = 7/2$, however, the hyperfine structure is not expected to be observed due to small values of the hyperfine structure parameters $\{A\}$ in the cluster and relatively large width of the EPR line. As follows from the typical A values for vanadium(IV) ion,[23] the A values for clusters with four magnetic ions should be of an order of 5–0.5 mT, whereas the observed ΔB was 46–15 mT. At the same time, the spin states of the exchange cluster of four ions with $S = 1/2$ showing EPR have integer values of the total spin and split due to the fine structure is expected. One can suppose that the expanded four-component spectrum is due to the states with $S = 2$, however, the fine structure of the EPR spectra from the states with $S = 1$ is absent and the reason for the appearance of the single line should be discussed separately.

We shall now consider some peculiarities and transformations of the EPR spectra, taking place upon temperature lowering. $\Delta B(T)$ and $g(T)$ of the predominant signal as well as the four-component spectrum view (Figs. 3, 7(a) and 7(b))

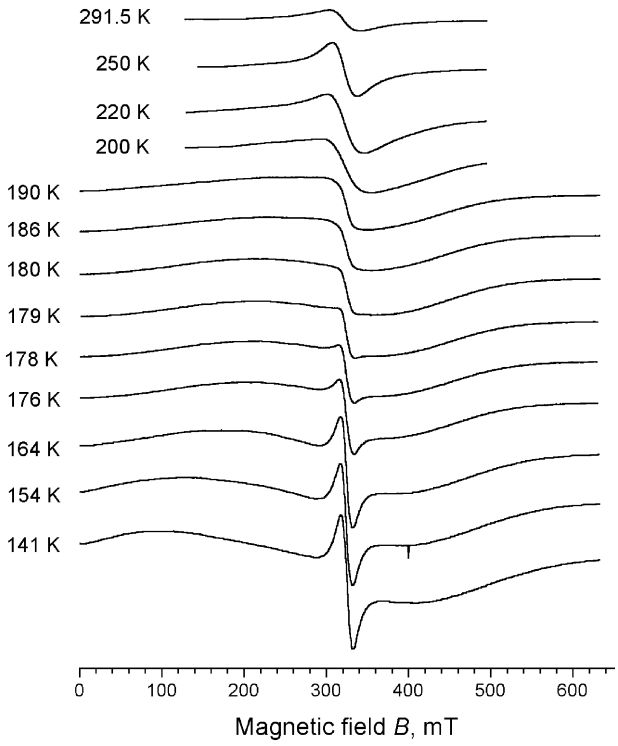

Fig. 3 The temperature evolution of the EPR spectrum recorded for the magnetic field B along [010] direction of the $[V_4^{IV}V_2^{V}O_7(OCH_3)_{12}]$ crystal.

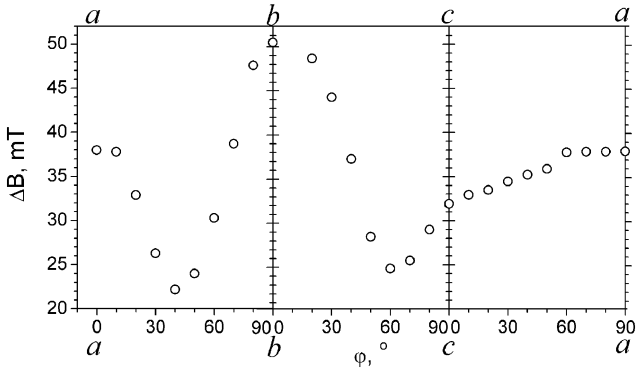

Fig. 4 The room-temperature angular dependences of the predominant resonance line width ΔB of the $[V_4^{IV}V_2^{V}O_7(OCH_3)_{12}]$ crystal.

will be analysed. The temperature dependences of ΔB, measured for various crystal orientations, are identical and differ only by the numerical ΔB values. The line width of the predominant single signal for $B \parallel [010]$ at $T = 291$ K is $\Delta B \approx 45$ mT ($g = 1.993 \pm 0.002$), diminishes to 38 mT ($g = 1.986 \pm 0.002$) at 250 K, before beginning to increase again with temperature decreasing to 200 K (Figs. 3 and 7). At these temperatures, the spectrum related to the $S = 2$ states also changes. The intervals between the EPR lines gradually increase, the spectrum becomes blurred and at about 190 K it becomes a broad expanded signal. Substantial transformation of the predominant signal and the expanded spectrum occurs in the range 200–170 K (see Fig. 3). The line widths and intensities of the expanded spectrum gradually grow and at 190–180 K the amplitude of the first derivative of the united signal becomes equal to that of the broadened single line. Then a rapid transformation of the spectrum takes place. At 178 K the narrow line with $\Delta B = 16$ mT (its g-factor is estimated at the middle point of the signal to about 1.985) and a distinct very broad signal with $\Delta B \approx 180$ mT appears instead of the four-component spectrum. It is necessary to note that the exact temperature interval of the rapid transformation of the spectrum differs in different crystals by several degrees. The subsequent temperature lowering to ~20 K does not lead to a visible change in ΔB of the narrow line, whereupon it increases to 4.2 K. The g-factor also changes. In contrast to the predominant signal behaviour, the broad signal "furl" of the fine structure spectrum becomes blurred again (as seen in Fig. 3) and has been not observed below ~130 K in comparable conditions down to ~10 K at which its trace was evidently observed on the low-field wing of the single signal.

The reversible changes in the whole spectrum were recorded upon temperature increase. The line width of the predominant EPR signal at 4.2 K was $\Delta B \approx 22$ mT and decreased with

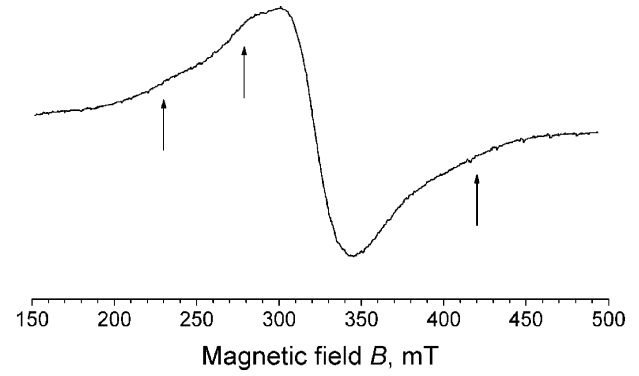

Fig. 5 EPR spectrum recorded for the magnetic field direction close to the [010] direction. Arrows indicate weak, additional signals originating from the state with $S = 2$.

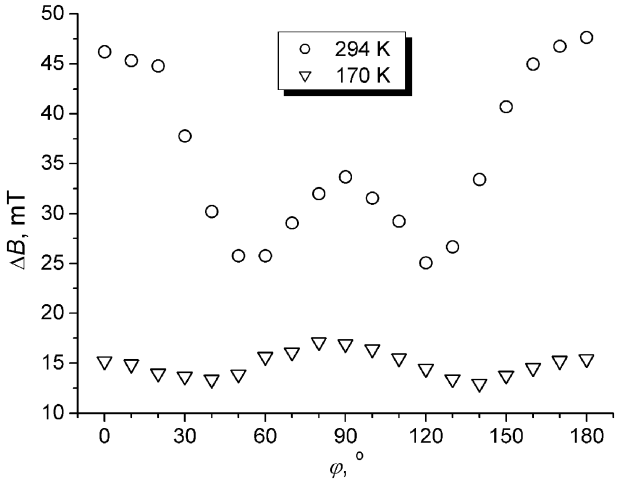

Fig. 6 Comparison of the angular dependences of the EPR line width ΔB of the predominant signal recorded in the (bc) plane at 294 K (○) and 170 K (△).

increasing temperature reaching 13.5 mT at 17 K, which was accompanied by a sharp increase in the g-factor from 1.965 at 4.2 K to 1.982 at 17 K (see Fig. 7(b)). In this temperature range, the signal intensity decreased, faster than expected from the Boltzmann law (Fig. 8). On heating, a kind of hysteresis was observed in the $\Delta B(T)$ dependence, but the parameters of the original spectrum were not reproduced and at room temperature: ΔB was about 33 mT. Similar $\Delta B(T)$ behaviour

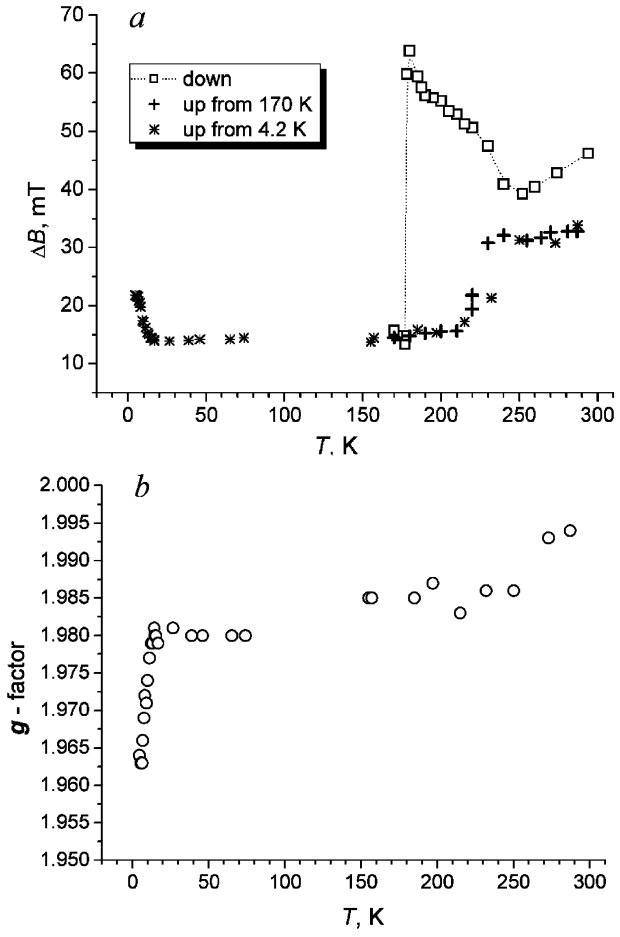

Fig. 7 Temperature dependences of the EPR predominant signal registered for the magnetic field orientation $B \parallel [010]$: (a) EPR line width ΔB (cooling from RT (□); heating from 170 K (+); heating from 4.2 K (*)) and (b) the g-factor values (on heating from 4.2 K).

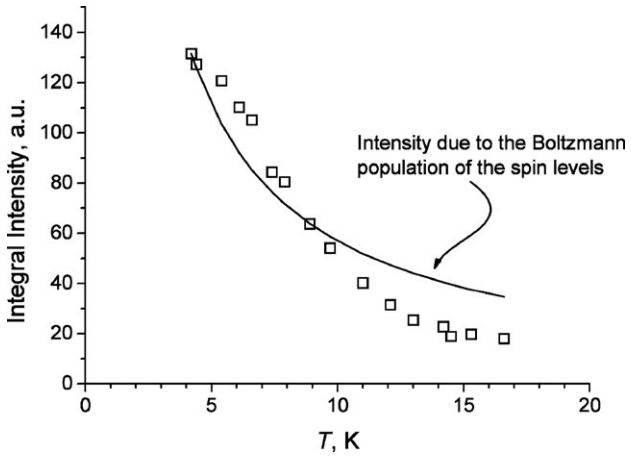

Fig. 8 Temperature dependence of the integral intensity of the EPR predominant signal.

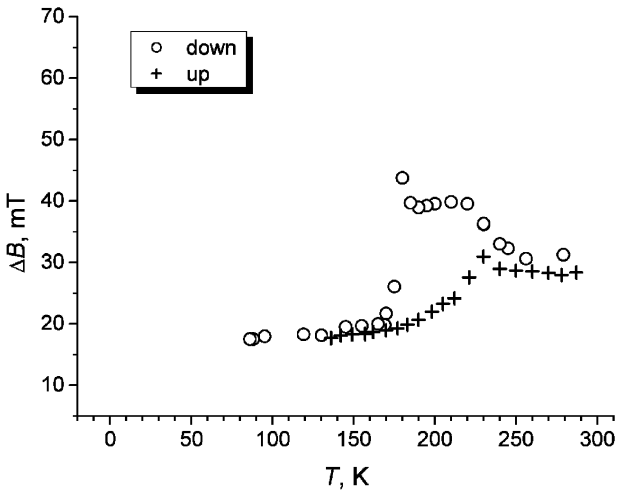

Fig. 9 Temperature dependence of the line width of the EPR signal registered for the magnetic field orientation $B \parallel [001]$

was observed for the $B \parallel [001]$ direction, although the range of ΔB changes was smaller (Fig. 9).

Discussion

Before starting the analysis of our results we would like to mention the features that should be explained for correct understanding of the general meaning of the observed facts. These are:

(a) The observation of EPR at room- and liquid helium-temperatures, as well as the coexistence of the predominant single signal and expanded spectrum in the entire temperature range.

(b) The nature of the predominant single signal.

(c) The angular dependences of the EPR spectra and their variation in the 291–165 K temperature range.

(d) The spectrum transformation observed in the 180–220 K temperature range.

(e) The uncorrelated behaviour of the line width ΔB of the predominant single EPR signal and the spectrum of the fine structure of the $S = 2$ state on decreasing temperature.

(f) The change in the g-factor in the 4.2–17 K temperature range.

(g) The temperature dependence of the predominant single signal's line width ΔB in the 4.2–291 K temperature range.

We begin with consideration of the possible electronic properties of the individual vanadium(IV) ions in the $[V_4^{IV}V_2^{V}O_7(OCH_3)_{12}]$ cluster. According to the V–O distances shown in Table 1, the V^{IV} ion is located in an octahedral crystal field with strong tetragonal distortion produced by the six surrounding oxygen ions. The bond lengths with the bridging oxygens are typical of the metal ion–oxygen σ-bonds (1.9043–2.0234 Å). At the same time the terminal oxygen bond lengths, (1.5811–1.5987 Å), are typical of the double covalent bonds with oxygen in vanadyl VO^{2+} complexes. The distances to the sixth, central oxygen atom (2.2175–2.3144 Å) are much longer. This displacement of the vanadium atoms away from the octahedron's central positions is characteristic of polyoxometalates and vanadium oxides.

Unfortunately, the EPR spectrum parameters of the isolated $V^{IV}O_6$ unit in the compound studied are inaccessible. Let us consider the parameters typical of the V^{IV} ion in an oxygen environment given in Table 2. An individual vanadium(IV) ion has the electron configuration $3d^1$, its ground term is ^2D, the electron spin $S = 1/2$, the nuclear spin $I = 7/2$. The values of the spectroscopic splitting factor g and of the hyperfine structure parameter A depend on the relationship between the values of ^2D-term splitting in the cubic crystal field Δ, the splitting of the low orbital triplet δ by lower symmetry crystal fields and the spin–orbital coupling parameter λ (the λ value for the free V^{IV} ion is ≈ 250 cm^{-1}) and can change in a relatively large interval (see Table 2).

It should be mentioned that $g_\parallel < g_\perp$ when vanadium is without doubt in the electron state VO^{2+} as in the case of the Tutton salt.[29] For the V^{IV} in TiO_2 and GeO_2 the value of $g_\parallel > g_\perp$ whereas in V_2O_5, $g_\parallel < g_\perp$. In the latter, the distances to the surrounding oxygen atoms are 1.58, 1.78, 1.86, 1.89, 2.02 and 2.79 Å, respectively.[28] A very short distance to one of the oxygen atoms combined with a very long distance to the opposite one as well as the axial symmetry of the g-factor, despite very low symmetry of the crystal field on the V-ion, allow a supposition of the VO^{2+} state. The presence of highly distorted VO^{2+} complexes in TiO_2 and GeO_2 crystals seems improbable due to the symmetry of the crystal host.[27] However, the conditions of the EPR signal observation are quite similar in the above-mentioned crystals. It is understandable why the EPR signal of VO^{2+} in various compounds is observed up to very high temperatures: a strong tetragonal ligand field leads to extremely large splitting of the lowest orbital ^2T-triplet which leads to long times of paramagnetic relaxation. In the discussed rutile type crystals conditions differ strongly and EPR studies of Ti^{III}, an ion with the same $3d^1$ electron configuration, confirm this statement. Strong spin–orbit

Table 2 EPR spectra parameters for the V^{IV} (and Ti^{III}) ion in selected compounds

	T/K	g_x	g_y	g_z	A_x/cm^{-1}	A_y/cm^{-1}	A_z/cm^{-1}	Ref.
V^{IV} in α-Al_2O_3	300	$g_\parallel \approx g_\perp = 1.97$			$A_\parallel = A_\perp = 0.000132$			24
V^{IV} in TiO_2	77	1.915	1.912	1.950	0.0031	0.0043	0.0142	25, 26
V^{IV} in GeO_2	300	1.921	1.921	1.963	0.003 669	0.003 754	0.013 436	27
V^{IV} in V_2O_5	77–300	$g_\perp = 1.98$, $g_\parallel = 1.82$			$A_\perp = 0.0046$, $A_\parallel = 0.0089$			28
VO^{II} in $Zn(NH_4)_2(SO_4)_2 \cdot 6H_2O$	290	1.9813	1.9801	1.9331	0.007 120	0.007 244	0.018 281	29
Ti^{III} in Al_2O_3	<9	$g_\perp = 0.1$, $g_\parallel = 1.067$						30
Ti^{III} in TiO_2	1.4	1.972	1.975	1.94				31

coupling leads to the relaxation times for the spin state belonging to the lowest orbital triplet ^2T being so short that EPR is only observable at very low temperatures. In V_2O_5:V^{IV} and GeO_2:V^{IV}, however, the EPR signal was studied without difficulties at 300 K; in TiO_2:V^{IV} at 77 K. (We should mention that in ref. 28 the V^{IV} spectra at 77 K are identical for both crystals.)

The given data do not allow a direct conclusion about the state of the V^{IV} ions and about EPR spectra parameters of individual ions in the compound studied. Results of the structural study support the idea that they are present as VO^{2+} ions. We should however remember, that only four from six vanadium ions are in a magnetic state and that the structure was determined at a relatively low temperature (173 K). Formally speaking, this temperature is lower than that of the sharp transformation of the EPR spectrum identified as a phase transition. At the same time, X-ray analysis of the structure at room- and low-temperature together with the stability of the studied crystals (a phase transition leads to crystal cracking) and some EPR results concerning the second cycle of transformation allow a supposition that the transition temperature depends on the grain size. Therefore, for small crystals used in structural determination the transition temperature can be lower than for those used in the EPR studies. Possibly, the data in question require additional study. We should keep these data in mind when considering the results obtained for the $[V_4^{IV}V_2^{V}O_7(OCH_3)_{12}]$ clusters and proceeding to their analysis.

In principle, the magnetic and spectroscopic behaviour of the $[V_4^{IV}V_2^{V}O_7(OCH_3)_{12}]$ exchange cluster depends on the positions of V^{IV} ions in the octahedron of vanadium ions. To start with, let us consider, according to the valence-sum calculations, their localization in the octahedron's equatorial positions, nearly coplanar to the *ac* crystal plane. In this case, interactions between ions 2 and 3, 3 and 4, 4 and 5 and 5 and 1 as well as between ions 2 and 4, and 3 and 5 can be considered as equivalent. The spin-Hamiltonian can thus be written as:

$$H = J_1[S_2S_4 + S_3S_5] + J_0[S_2S_3 + S_3S_4 + S_4S_5 + S_5S_2] + H_z + H_{fs} + H_{hfs}, \quad (1)$$

where $S_i = 1/2$ (index marks in S_i correspond to notations on Fig. 1), J_i are the parameters of the isotropic exchange interactions between the corresponding V^{IV} ions and H_z, H_{fs} and H_{hfs} describe the interaction of the vanadium ions with the magnetic field, the zero-field splitting of the spin levels and the hyperfine interactions, respectively, which lead to the corresponding structures of the EPR spectrum. The total spin of the cluster S is obtained according to the quantum mechanical rules, which consist in adding up the individual spins *via* the S_{24} and S_{35} intermediates. The total, intermediate, and individual spin operators in eqn. (1) commute, leading to the solution of the exchange Hamiltonian:

$$E/|J_0| = J_1/|J_0|[S_{24}(S_{24}+1) + S_{35}(S_{35}+1) - 3] + [S(S+1) - S_{24}(S_{24}+1) - S_{35}(S_{35}+1)]. \quad (2)$$

The spin states consist of one quintet ($S = 2$), three triplets ($S = 1$) and two singlets ($S = 0$). The signs and values of the J_i parameters determine their relative energies and it is useful to use the so-called correlation diagram for their presentation. Such a diagram, presented in Fig. 10, shows that in the case of antiferromagnetic exchange (J_1 and $J_0 > 0$), which can be assumed for the clusters in question, the lowest spin states have $S = 0$ for all values of the $J_1/|J_0|$ ratio and at $T = 4.2$ K the EPR should not be observed. Even in the case of very small J_i when the $E|S,S_{24},S_{35}\rangle = E|110\rangle$, $E|101\rangle$ and $E|111\rangle$ states would populate, the temperature dependence of the spectrum would differ form the observed one. (Supposing ferromagnetic exchange would lead to a very strong temperature dependence of spectrum, which is also not consistent with the dependence observed).

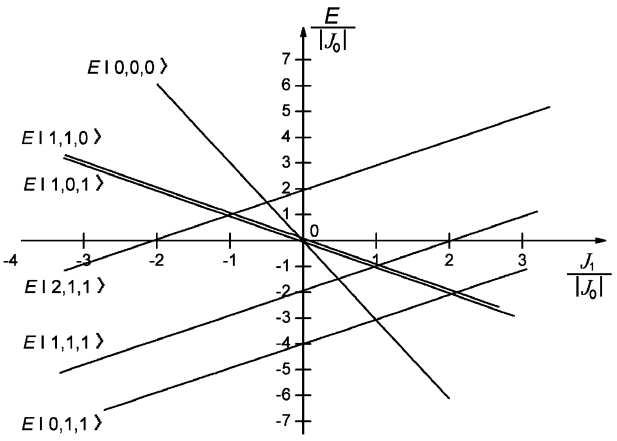

Fig. 10 A diagram showing the dependence of the energy of spin states of the cluster on the ratio of values of the exchange parameters J_1 and J_0.

We can also consider two other localizations of V^{IV} ions. In one of them four magnetic ions adopt a "butterfly" configuration (V^{IV} ions occupy, for example, positions V_2, V_4, V_1 and V_6). The exchange Hamiltonian is then similar to (1), but has different exchange parameters for the S_2S_4 and S_1S_6 pairs. The degeneracy over intermediate spins is then completely cancelled. However, if individual exchange parameters are antiferromagnetic, the ground state can only be a singlet. The third possible localization of V^{IV} ions is realized when three equivalent ions occupy the corners of a square and the fourth one is in one of two external apexes. We can write the exchange Hamiltonian for this localization in the form:

$$H = J_1S_2S_4 + J_0[S_2S_3 + S_3S_4 + S_1S_2 + S_1S_3 + S_1S_4]. \quad (3)$$

(We neglect here the possible difference in exchange coupling between S_2S_3 and S_1S_2). It can be easily shown that this Hamiltonian is mathematically identical to that obtained for the "butterfly" configuration. All this means that the approximation of the isotropic exchange alone does not allow an interpretation of the observed spectrum.

Until now we have neglected the possibility of excess electron transfer between neighbouring V^{IV} and V^{V} sites. In the simple case of two ions in different oxidation states (the so called two ion–one electron problem), the approach assuming the equivalence of the V^{IV}–V^{V} and V^{V}–V^{IV} states of the pair of ions should lead to the degeneracy of these states. This degeneracy is cancelled, resulting in the splitting of the spin states of the pair.[2,3] Solving the problem of excess electron transfers in the hexanuclear $[V_4^{IV}V_2^{V}O_7(OCH_3)_{12}]$ cluster is more complicated and will be analysed separately. Here we only take into account the main ideas of this phenomenon, which help to understand the experimental results.

Four extra electrons can be distributed between six metallic centres in 15 ways, thus defining the degeneracy of each spin state. Taking into account the electron delocalisation leads to a splitting of all spin states. The character of this splitting depends on: (1) the total spin value, (2) the cluster symmetry (ideal octahedron or distorted octahedron), (3) the basic interactions taken into account (only electron delocalisation, electron delocalisation + intra- and/or inter-centre electronic repulsions, *etc.*). Preliminary analysis shows that for the ideal octahedral symmetry, when taking account electron delocalisation only, each spin level is split into one singlet, one doublet, two triplet, and one sextet level. However, such relatively simple conceptions are further complicated by the fact that the considered electron localization patterns are described by different Heisenberg Hamiltonians. Taking into account the possibility of hopping between different schemes of exchange

interaction we get a mixing of states with the same spin but characterized by different intermediate spin values. It is possible that this mixing process, in combination with the splitting of the states, stabilizes a triplet ground state.

Until now we used as the starting point the picture of four localized electronic spins. However, a non-zero spin ground state can also follow from the opposite limiting case of delocalised electronic states within the MO model description. If we consider that each vanadium centre provides a single localized orbital, which can be singly populated by a transferred electron, the simple Hückel Hamiltonian within this basis will result in three molecular orbitals. The energies of these orbitals are $4t$ (non-degenerated), 0 (triply degenerated), and $-2t$ (doubly degenerated), where t is the transfer parameter. If t is negative, which is usually the case, two delocalised electrons occupy the lowest non-degenerated orbital, whereas the two remaining electrons will stay at the triply degenerated orbital. According to Hund's rule, this partial occupation of the degenerated orbital should result in a triplet ground state. One can say that in terms of the delocalised description, a magnetic ground state results from an idealized topology of the cluster and a particular filling of electronic levels.

Below we shall discuss the experimental results in the phenomenological approach of the model exchange Hamiltonians (1) and (3) taking into account the splitting of the energy states of type (2) degenerated due to different possible distributions of magnetic electrons between metal sites. The splitting is due to transfers of the V^{IV} extra electrons. The transitions between some possible configurations of the V^{IV} ions in the V_6 cluster will be also considered.

We can accept the localization of V^{IV} ions in the equatorial positions of V_6-cluster as the most probable one and consider the electron transfers keeping in mind the deviation of the V_6 octahedron from the ideal form. To understand the EPR observation down to the lowest temperatures and the fact that the largest intensity of the whole EPR spectrum corresponds to $T = 4.2$ K (see Fig. 8), we should assume that the splitting of the total spin S states due to electron transfers should be comparable to and somewhat greater than J. Among the possible electron transfers the most probable are those of extra electrons of V^{IV}_{2-5} ions onto the apical V^{IV}_{1-6} ions. These very transitions are supposed to lead to the new composition of the total spin states, with the states of $S = 1$ being the lowest ones.

Let us consider now an origin of the observed EPR signals. It is convenient to subdivide the spectrum observed into the predominant single signal (only its line width ΔB and g-factor change with temperature) and the expanded spectrum, which varies in the temperature intervals 290–200 K (four separate broad lines with interval changing with temperature), 200–130 K (broad EPR line or a broad signal with unresolved structure) and 130–4.2 K (hardly detectable EPR signals). As mentioned in the previous section, the EPR signals observed in 290–200 K (see Figs. 3 and 5) can be attributed to transitions within the spin multiplets with $S = 2$. In the magnetic field, the intervals between these signals allow estimation of the fine-structure parameter $D_{(quintet)} \approx 0.03$ cm^{-1}. The whole extension of the EPR spectrum for the $S = 2$ state (including the contribution due to the hyperfine structure) is about 0.18 T. One can consider that the fine-structure parameters of the $S = 2$ and $S = 1$ states are comparable, *i.e.* $D_{quintet} \approx D_{triplet}$. This means that the extension of the spectrum for the state $S = 1$ should be of about 0.06 T. Instead, we observe a single EPR line. The crystal structure of the $[V^{IV}_4V^{V}_2O_7(OCH_3)_{12}]$ compound and absence of chemical contacts between clusters allow excluding the possibility of inter-molecular exchange interaction. The uncorrelated changes of the line width ΔB of the predominant signal and of the spectrum of the $S = 2$ states with temperature confirm this conclusion. The only reason for the appearance of the predominant signal is the existence of a certain dynamic averaging of the fine structure of $S = 1$ states. This dynamics can be connected with the transitions between different configurations of the mixed-valence cluster. In other words, we suppose that the predominant single EPR signal represents the states with $S = 1$, whose fine structure is averaged due to the electron transitions at the rate $\nu_{tr} > 2D_{triplet}/h$. (Here $2D_{triplet}$ is the spectrum extension for magnetic field B parallel to V_1–O–V_6 direction. Deviation of these directions of the four crystallographic equivalent clusters from the b axis to the angle $\theta = 12^\circ$ decreases the spectrum extension to $\cos\theta$ and is not significant). It can be supposed that in the temperature interval 291–200 K the value $\nu_{tr} \approx (0.5–0.6) \times 10^{10}$ s^{-1} is sufficient for averaging the fine structure of the $S = 1$ states, however, it is not sufficient for averaging the fine structure of the spectrum of the $S = 2$ states, which is at least three times more extended.

The electron transfers giving rise to the new composition of the total spin states are single jumps ones that result in the eight new configurations of the V^{IV} ions. In principle, the transitions between these configurations represent the double-jump processes and they can be assumed to have a lower frequency and be responsible for the cluster dynamics. However, it is not quite clear how to choose the main symmetry axes for the such V^{IV} configurations: the plane V_i–O_{centr} or perpendicular V_1–V_6 directions seem to be very similar and the mixing of configurations, for example, with V_1–V_6 main axes would not lead to the averaging of the fine structure of the EPR spectra. And so, we should keep in mind the possibility of simultaneous transfers of the extra electrons of the plane $V_{2(3)}$ and $V_{4(5)}$ ions onto the orbitals of V_1 and V_6 ions.

The temperature dependence of the single line width ΔB and the four-component spectrum for $T > 200$ K and for $T < 170$ K can be considered as the evidence confirming that the transition rate ν_{tr} is different for the averaging of the different V^{IV}–V^{V} configurations in the $[V^{IV}_4V^{V}_2O_7(OCH_3)_{12}]$ cluster, taking part in the electron transfers phenomenon (the temperature interval 200–170 K will be considered separately. The possible differences in the energy of different configurations follow from the differences in the electron transfer energies due to the small changes in the structure parameters of the V_i–$O_{1(6)}$ units (see Table 1). At the same time one can estimate the value of the exchange parameters J, neglecting the differences in J_0 and J_1 in eqn. (2): it should be of an order of $\sim$150–200 cm^{-1} to show the temperature behaviour of the EPR signal intensities.

The width of the observed EPR lines is determined by the (i) anisotropic part of V^{IV}_i–V^{IV}_j exchange interactions and magnetic dipole–dipole interactions of V^{IV} ions in the cluster leading to definite values of D parameters, (ii) by the definite splitting of the fine-structure signals due to hyperfine interactions and (iii) by the rate of the unpaired electron migration ν_{tr}. All these interactions, except that giving ν_{tr}, are strongly anisotropic (see Table 2) and lead to the definite dependence of the EPR spectrum or the EPR line width, resulting after its averaging, from the angle θ between the constant magnetic field and the cluster axis of symmetry. Taking into account a very small deviation of the main axes of the magnetic inequivalent clusters relative to the b axis we could expect a large anisotropy of ΔB (and g-factor of the EPR signal as well) for the rotation of magnetic field in the bc and ab planes. Such an anisotropy is readily observed for both the predominant EPR signal (see Fig. 4) and the four-component spectrum. The minimum value of ΔB for the B-direction for $\theta = 54^\circ$ is the evidence of the main contribution to ΔB coming from the spin–spin interactions.

We can see that the approach described above allows an explanation of the features of the experimental spectra behaviour denoted as (a)–(c) and (e) in the beginning of this section. Let us come to the temperature dependence of the g-factor, mainly in the 4.2–17 K temperature range (features denoted by (f) and (g), see Fig. 7(b)), accompanied by the $\Delta B(T)$ dependence in this temperature interval, which is an intriguing observation. In principle, the $g(T)$ dependence for a given

direction of the static magnetic field is also observed for other temperatures. However, more states with $S = 1$ can contribute to the observed EPR signal at higher temperatures, which is less convenient for analysis.

Using the approximation of Hamiltonian (1) and keeping in mind the splitting of the spin states due to electron transfer, we could consider the observed predominant signal as originating from transitions within the $E|110\rangle$, $E|101\rangle$ and $E|111\rangle$ states having low and high energy (Fig. 10 should be modified by the splitting of the spin levels). The analysis, analogous to the one carried out in ref. 32 for three nuclear cluster, shows that EPR on the $E|110\rangle$, $E|101\rangle$ and $E|111\rangle$ states should occur with different g-values due to differences in the intermediate spins. Indeed, in accordance with[32] one can obtain the following expression for the cluster g-factor (for $B \parallel V_2$–O_{centr}–O_4 direction):

$$g = (g^i_{\parallel} + g^i{}_{\perp})/2 + (g^i_{\parallel} - g^i{}_{\perp})[S_{24}(S_{24}+1) - S_{35}(S_{35}+1)]/2S(S+1). \quad (4)$$

As follows from the expression (4), the cluster g-factor depends on the value of intermediate spins S_{24} and S_{35}. This means that, for example, for $g^i_{\parallel} < g^i{}_{\perp}$ (where $g^i_{\parallel}$ and $g^i{}_{\perp}$ are the components of the g-factor of individual ions) the cluster g-factor for the state $E|1,1,1\rangle$ should differ from g-factor for the states $E|1,0,1\rangle$ and $E|1,1,0\rangle$ on $|(g^i_{\parallel} - g^i{}_{\perp})/2|$ (modified Fig. 10: the states of $S = 1$ are lower than the states of $S = 0$ due to the splitting of the spin levels caused by the electron transfers and in correspondence with the obtained results).

Taking into account that even very small distortions of the cluster removes degeneracy of the $E|1,0,1\rangle$ and $E|1,1,0\rangle$ states, we can obtain the following order of the lowest energy levels: $E|1,1,0\rangle$ is lower than $E|1,1,1\rangle$ lower than $E|1,0,1\rangle$ or $E|1,1,0\rangle$ is lower than $E|1,0,1\rangle$ lower than $E|1,1,1\rangle$ (the difference in the g-factors for $E|1,0,1\rangle$ and $E|1,1,0\rangle$ states is the same , according to (4), $\Delta g = (g^{ind}_{\parallel} - g^{ind}_{\perp})$). As shown in Fig. 8, a decrease in the signal integral intensity with increasing temperature in the range 4.2–17 K is more rapid than would be expected from the Curie law. This means that a state or states with $S = 0$ or $S = 2$ can also be populated upon temperature increase.

The experimental results were considered assuming that the structure parameters are invariable with temperature. In reality, the complex properties of the $[V^{IV}_4V^{V}_2O_7(OCH_3)_{12}]$ cluster are additionally complicated due to transformations of the crystal lattice and molecule dynamics occurring in the vicinity of 180 K. The transformation, shown in Fig. 7, can be interpreted as a first order phase transition with a significant hysteresis.

A change in the character of the angular dependence of the line width ΔB at $T = 170$ K, just below the phase transition temperature, shown in Fig. 6, responsible for a change in the directions of the largest and intermediate line widths ΔB of the predominant signal (see description of the experimental results), indicates that phase transition is accompanied by a change in the initial localization of the V^{IV} ions. The preferable sites are now $V_2V_1V_4V_6$. The changes in the character of the angular dependences are accompanied by narrowing of the observed EPR signal, which is strongest in the direction of the b axis. It can be supposed that the transition to the low-temperature phase leads to an increase in the migration rate of additional electrons and results in narrowing of the single EPR line for the state or states with $S = 1$ (as shown in Figs. 3 and 7(a), ΔB decreases from $\approx$40 mT at $T = 250$ K to $\approx$18 mT at 180 K) and in averaging of the fine structure of the spectrum for the state with $S = 2$ into one broad line (see Fig. 3). Estimation of parameter D on the basis of the spectrum's appearance (Figs. 3 and 5) as $D \approx 0.08$–0.1 cm^{-1} allows a conclusion that for $T < 180$ K the transition frequency ν_{tr} is of about 10^{10} s^{-1}.

The increase in the predominant single signal line width ΔB from $\approx$40 mT at 250 K to over 60 mT at 200 K (Fig. 7(a)), as well as its blurring in the 200–180 K range, above the phase transition temperature (Figs. 3 and 7(a)), are both very interesting observations. The line width increase by about 40 mT cannot be attributed to the population of the spin states characterized by different g-factors. It would require $\Delta g\beta B \approx 0.3$ cm^{-1} instead of the observed value of approximately 0.01–0.02 cm^{-1}. We assume that in the compound studied there is a deceleration of some vibration modes or some dynamical processes take place in the vicinity of the critical region of the phase transition.[33,34]

Conclusion

Paramagnetic resonance allows observation of the states of the cluster with $S = 2$ and $S = 1$. An averaging of the spectrum of the states with $S = 1$ indicates some kind of motion in the compound studied. The exchange interactions between magnetically inequivalent complexes have been shown to be too weak to cause an averaging of the spectra and we have come to a conclusion about the existence of definite intramolecular dynamical processes. Analysis of the EPR spectra recorded over a wide temperature interval (300–4.2 K) indicates the presence of states with both $S = 1$ and 2 among the low and high energy spin states of the cluster.

Thus, we can conclude that paramagnetic resonance of the mixed-valence cluster $[V^{IV}_4V^{V}_2O_7(OCH_3)_{12}]$ containing four V^{IV} ions with an electron spin $S_i = 1/2$ has shown that the Heisenberg–Dirac–Van Vleck approach of the isotropic exchange interactions together with the transfer phenomenon of extra electrons on the empty orbitals of non-magnetic V^{V} ions in principal clears the way for understanding the experimental facts. However the problem remains complex.

The system in question consists of six centres and four electrons, and conception of the resulting spin density distribution at different vanadium ions is important in solving the problem of the cluster properties. One of the questions, which we would like to clarify, concerns the structure of the cluster molecule and the electronic structure of the individual VO_6 complex. The $[V^{IV}_4V^{V}_2O_7(OCH_3)_{12}]$ cluster includes magnetic and nonmagnetic VO_6 complexes, which can have different configurations depending on the chemical bond character, mainly the terminal oxygen atom. This means that the electron dynamics is accompanied by a specific dynamics of the molecule.

Formally speaking, the cluster molecule has a highly symmetric structure, however the symmetry of the crystal is not high, and VO_6 octahedrons show different distortions. The results obtained allow a supposition that these distortions are connected with packing effects of the molecules in the crystal, and with effects connected with energy differences in the different dynamical configurations. The latter conclusion is based on a relatively small splitting of spin multiplets due to electron transfer, and a large number of spin states populated in the entire temperature range of measurements. In this respect, the phase transition discovered in the compound studied is of special interest. The elucidation of the type of vibrational processes quenched upon temperature lowering would be useful for better understanding of the spin and molecular dynamics in $[V^{IV}_4V^{V}_2O_7(OCH_3)_{12}]$.

References

1 P. W. Anderson, in *Magnetism*, ed. G. T. Rado and H. Shuhl, Academic Press, New York, 1963, vol. 1, ch. 2.
2 C. Zener, *Phys. Rev.*, 1951, **82**, 4093.
3 P. W. Anderson and H. Hasegawa, *Phys. Rev.*, 1955, **100**, 675.
4 G. Blondin and J.-J. Girerd, *Chem. Rev.*, 1990, **90**, 1359.
5 G. Blondin, S. Borshch and J.-J. Girerd, *Comments Inorg. Chem.*, 1992, **12**, 315.

6 E. L. Bominaar, S. A. Borshch and J.-J. Girerd, *J. Am. Chem. Soc*., 1994, **116**, 5362.
7 J. J. Girerd and J. P. Launay, *Chem. Phys*., 1983, **74**, 217.
8 S. A. Borshch and B. Bigot, *Chem. Phys. Lett*., 1993, **212**, 398.
9 (*a*) J. J. Borrás-Almenar, J. M. Clemente, E. Corronado and B. S. Tsukerblat, *Chem. Phys*., 1995, **195**, 1; (*b*) J. J. Borrás-Almenar, J. M. Clemente, E. Corronado and B. S. Tsukerblat, *Chem. Phys*., 1995, **195**, 17; (*c*) J. J. Borrás-Almenar, J. M. Clemente, E. Corronado and B. S. Tsukerblat, *Chem. Phys*., 1995, **195**, 29.
10 H. Duclusaud and S. A. Borshch, *J. Am. Chem. Soc*., 2001, **123**, 2825.
11 N. Suaud, A. Gaita-Ariño, J. M. Clemente-Juan, J. Sánchez-Martin and E. Coronado, *J. Am. Chem. Soc*., 2002, **124**, 15134.
12 V. Barone, A. Bencini, I. Ciofini, C. A. Daul and F. Totti, *J. Am. Chem. Soc*., 1998, **120**, 2357.
13 N. Guihery and J. P. Malrieu, *J. Chem. Phys*., 2003, **119**, 8956.
14 R. D. Willett, D. Gatteschi and O. Kahn, in *Magneto-Structural Correlations in Exchange Coupled Systems Mixed Valence Compounds*, ed. D. B. Brown, Reidel, Dordrecht, The Netherlands, 1980.
15 Yu. V. Yablokov, V. K. Voronkova and L. V. Mosina, *Paramagnetic Resonance of Exchange Clusters*, Nauka, Moscow, 1988 (in Russian).
16 D. Gatteschi and A. Bencini, *Electron Paramagnetic Resonance of Exchange Clusters*, Springer, Berlin–Heidelberg, 1990.
17 S. A. Borshch, I. N. Kotov and I. B. Bersuker, *Chem. Phys. Lett*., 1984, **111**, 264.
18 V. Z. Polinger, L. F. Chibotaru and I. B. Bersuker, *Mol. Phys*., 1984, **52**, 1271.
19 V. K. Voronkova, J. Mrozinski and Yu. V. Yablokov, *Z. Phys. Chem*., 1997, **201**, 181.
20 M. J. Manos, A. J. Tasiopoulos, E. J. Tolis, N. Lalioti, J. D. Woollins, A. M. Slawin, M. P. Sigalasans and T. A. Kabanos, *Chemistry*, 2003, **9**, 695.
21 J. Spandl, C. Daniel, I. Brűdgam and H. Hartl, *Angew. Chem., Int. Ed*., 2003, **42**, 1163.
22 N. E. Brese and M. O'Keeffe, *Acta Crystallogr., Sect. B*, 1991, **47**, 192–197.
23 S. A. Al'tshuler and B. M. Kozyrev, *Electron Paramagnetic Resonance in Compounds of Transition Elements*, Wiley, New York, 2nd edn., 1974.
24 J. Lambe and C. Kikuchi, *Phys. Rev*., 1960, **118**, 71.
25 H. J. Gerritsen and H. R. Lewis, *Phys. Rev*., 1960, **119**, 1010.
26 (*a*) G. M. Zverev and A. M. Prohorov, *J. Exp. Theor. Phys. Russ*., 1960, **39**, 222; (*b*) G. M. Zverev and A. M. Prohorov, *JETP Lett (Engl, Transl.)*, 1961, **12**, 160.
27 I. Siegel, *Phys. Rev. A*, 1964, **134**, 193.
28 V. A. Ioffe and I. B. Patrina, *Solid State Physics, Russ*., 1964, **6**, 3045.
29 R. H. Borcherts and C. Kikuchi, *J. Chem. Phys*., 1964, **40**, 2270.
30 L. S. Kornienko and A. M. Prohorov, *J. Exp. Theor. Phys., Russ*., 1960, **38**, 1951.
31 H. S. Jarrett, *J. Chem. Phys*., 1957, **27**, 1298.
32 (*a*) Yu. V. Yablokov, V. A. Gaponenko, M. V. Eremin, V. V. Zelentsov and T. A. Jzemchujznikova, *J. Exp. Theor. Phys., Russ*., 1973, **65**, 1979; (*b*) Yu. V. Yablokov, V. A. Gaponenko, M. V. Eremin, V. V. Zelentsov and T. A. Jzemchujznikova, *JETP Lett. (Engl. Transl.)*, 1974, **38**, 988.
33 G. F. Reiter, W. Berlinger and K. A. Műller, *Phys. Rev. B: Condens. Matter*, 1980, **21**, 1.
34 K. A. Műller and W. Berlinger, *Z. Phys. B*, 1978, **31**, 151.